

## Electron-hole plasma dynamics in CdTe in the picosecond regime

J. H. Collet

*Laboratoire de Physique des Solides, Institut National des Sciences Appliquées,  
avenue de Rangueil, 31077 Toulouse CEDEX, France  
and Max-Planck-Institut für Festkörperforschung, Heisenbergstrasse 1, D-7000 Stuttgart 80, Federal Republic of Germany*

W. W. Rühle

*Max-Planck-Institut für Festkörperforschung, Heisenbergstrasse 1, D-7000 Stuttgart 80, Federal Republic of Germany*

M. Pagnet

*Laboratoire de Physique des Solides, Institut National des Sciences Appliquées,  
avenue de Rangueil, 31077 Toulouse CEDEX, France*

K. Leo\*

*Max-Planck-Institut für Festkörperforschung, Heisenbergstrasse 1, D-7000 Stuttgart 80, Federal Republic of Germany*

A. Million

*Laboratoire d'Électronique et de Technologie de l'Informatique, Commissariat à l'Énergie Atomique,  
avenue des Martyrs, 85X 38041 Grenoble, France*

(Received 30 June 1989)

The relaxation of photogenerated electron-hole plasmas is investigated in CdTe using time-resolved luminescence in the picosecond regime. The plasma temperature, the plasma density, and the band-gap renormalization are traced during the relaxation following the excitation pulse. Transient luminescence spectra are analyzed, first in a mostly used free-particle model and second, including carrier collision broadening calculated in the plasmon-pole approximation. The transient temperatures obtained with the second presumably correct model prove to be significantly lower. The plasma cooling is slowed down with increasing initial plasma density. The temperature decay is compared to plasma cooling theory including hot-phonon effects. The agreement is satisfactory for the densities ranging from  $5 \times 10^{16} \text{ cm}^{-3}$  to  $4 \times 10^{17} \text{ cm}^{-3}$ . Additionally, good agreement is found between our experimental results of band-gap shrinkage and theory. This work represents the first simultaneous test of several aspects of the electron-hole plasma theory including the many-body line-shape theory, the quasiparticle damping, the band-gap renormalization, and the plasma cooling kinetics.

### I. INTRODUCTION

CdTe,  $\text{Cd}_x\text{Zn}_{1-x}\text{Te}$ , and  $\text{Cd}_x\text{Hg}_{1-x}\text{Te}$  are II-VI compounds which are of interest for the development of new optoelectronic devices for infrared light emission or absorption. This interest is stimulated both by recent progress in molecular-beam epitaxy of these materials as well as by their possible use in all-optical modulation in relation with all-optical data-processing techniques.<sup>1,2</sup> In these techniques, the transmission of thin platelets is modulated by changes in the state (i.e., density and temperature) of a generated high-density electron-hole plasma (EHP). The concomitant change of the optical properties such as induced absorption or transmission are strongly nonlinear and decay generally on a subnanosecond time scale following a picosecond laser-pulse excitation. To our knowledge, only a few investigations have been published on EHP in CdTe. The plasma expansion and the band-gap renormalization have been investigated in Ref. 3, whereas the time and density depen-

dence of the exciton-polariton has been investigated in Ref. 4.

The aim of the present paper is twofold. First, we try to close the gap between basic experimental and theoretical investigations on the dynamics of high-density EHP in CdTe in the picosecond regime, and to elucidate its importance for possible future applications. Second, we reveal a serious problem which arises if, as usually done, many-body effects are neglected when determining the temperature out of the experimentally detected transient luminescence spectra. This second point is of general interest and the consequences are not restricted to the case of CdTe. Very often, the EHP temperature is simply extracted from a quasiexponential high-energy tail of the radiative luminescence spectra.<sup>5-13</sup> Here we extend the analysis to fit the whole line shape using many-body theories and including in particular the collision broadening,<sup>14,15</sup> i.e., the broadening of electronic states by emission and absorption of plasmons as well as the participation of plasmons in optical transitions. The temperatures

deduced by this new advanced method prove to be appreciably lower than those determined from the simpler, more naive single-particle description.

We compare the EHP cooling kinetics with a theory of phonon emission and absorption which includes the distortion of the phonon distribution by the strong generation of phonons during the EHP cooling process (i.e., the so-called *hot-* or *nonthermal-*phonon effect). Satisfactory agreement is found for the densities ranging from  $5 \times 10^{16} \text{ cm}^{-3}$  to  $4 \times 10^{17} \text{ cm}^{-3}$ . The band-gap renormalization deduced from the line-shape fits is in good agreement with the theory developed by Zimmermann.<sup>16</sup>

## II. EXPERIMENTAL RESULTS

The samples are thin layers of CdTe grown by molecular-beam epitaxy on a  $\text{Cd}_{0.96}\text{Zn}_{0.04}\text{Te}$  substrate. Substrate growth rate was  $1 \mu\text{m/h}$  at the temperature of  $300^\circ\text{C}$  using one CdTe cell as a source. The  $\text{Cd}_x\text{Zn}_{1-x}\text{Te}$  substrate has the advantages of a very small lattice mismatch with CdTe (0.2%), a relatively good crystal quality, and a band-gap energy which is about 20–25 meV larger than that of CdTe. The CdTe epitaxy thickness was  $0.8 \mu\text{m}$ . The absorption coefficient is about  $5 \times 10^4 \text{ cm}^{-1}$  (Ref. 17) so that the plasma is not homogeneous in the direction perpendicular to the excited surface. Note, however, that diffusion tends to homogenize the plasma because of the blocking barrier of  $\text{Cd}_x\text{Zn}_{1-x}\text{Te}$ . The plasma density will be determined directly from the luminescence line-shape analysis. The samples are mounted on the cold finger of a He cryostat and excited by a synchronously pumped mode-locked dye laser with a repetition rate of 80 MHz and a pulse length of 4–6 ps [full width at half maximum (FWHM)]. The luminescence is spectrally dispersed by a 0.32-m mono-

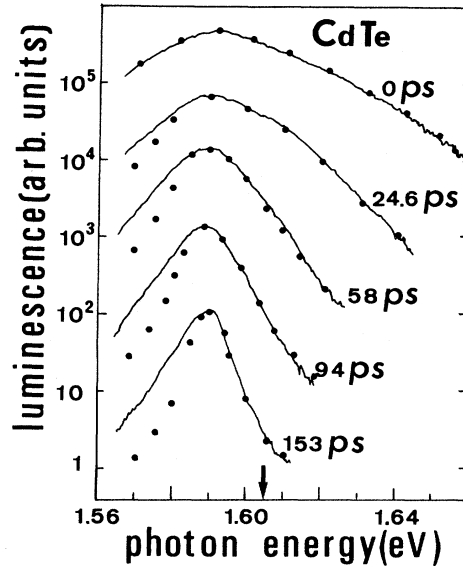


FIG. 1. Time-resolved picosecond luminescence of a CdTe epitaxy layer on a  $\text{Cd}_x\text{Zn}_{1-x}\text{Te}$  substrate. Lattice temperature is about 10 K. Excitation photon energy is 1.7 eV. Parameters deduced from the line fits for different delays are delay 0 ps, density  $\rho \approx 4 \times 10^{17} / \text{cm}^3$ , temperature 110–120 K; delay 24.6 ps, density  $\rho \approx 4 \times 10^{17} / \text{cm}^3$ , temperature 70 K; delay 58 ps, density  $\rho \approx (2.4-3) \times 10^{17} / \text{cm}^3$ , temperature 40 K; delay 94 ps, density  $\rho \approx 1.5 \times 10^{17} / \text{cm}^3$ , temperature 30 K; delay 153 ps, density  $\rho \approx (0.5-1) \times 10^{17} / \text{cm}^3$ , temperature 20–25 K.

chromator and additionally temporally resolved by a two-dimensional streak camera. The overall time resolution is better than 20 ps. The excitation photon energy is chosen to be 1.70 eV. All the material parameters used in

TABLE I. Experimental parameters.

	CdTe	CdSe	GaAs
Band gap (eV) at $T=4 \text{ K}$	1.6053	1.841	1.502
Electron effective mass	0.1	0.13	0.066
Hole effective mass	0.4	0.8	0.57
Exciton building energy (MeV)	9.4	16.5	4.1
$\epsilon_\infty$	7.1	6.3	10.63
$\epsilon_0$	10.5	9.4	12.56
LO-phonon energy (meV)	21.3	26	36.7
TO-phonon energy (meV)	17.4		33.3
Optical deformation potential (eV/cm)	$10^9$		$10^9$
Acoustical deformation potential (eV)			
electrons	5	3.7	7
holes		5.7	3.5
Mean sound velocity (cm/s)	$3.39 \times 10^5$	$2.3 \times 10^5$	$3.5 \times 10^5$
Piezacoustic factor	$2.8 \times 10^{-3}$	$2.6 \times 10^{-2}$	$4.2 \times 10^{-3}$
Density ( $\text{g/cm}^3$ )	5.85	5.68	6.75

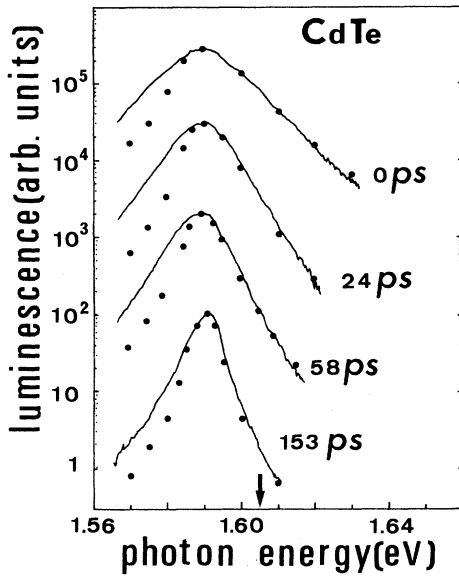


FIG. 2. Time-resolved picosecond luminescence of a CdTe epitaxy layer on a  $\text{Cd}_x\text{Zn}_{1-x}\text{Te}$  substrate. Lattice temperature is about 10 K. Excitation photon energy is 1.7 eV. Parameters deduced from the line fits for different delays are delay 0 ps, density  $\rho \approx (0.7-1) \times 10^{17}/\text{cm}^3$ , temperature 60 K; delay 24.6 ps, density  $\rho \approx (0.7-1) \times 10^{17}/\text{cm}^3$ , temperature 30–35 K; delay 58 ps; density  $\rho \approx (5-7) \times 10^{16}/\text{cm}^3$ , temperature 25–30 K; delay 153 ps; density  $\rho \approx (2.5-5) \times 10^{16}/\text{cm}^3$ , temperature 15–20 K.

the analysis of the experimental results are listed in Table I. Typical time-resolved luminescence spectra are displayed in Fig. 1. The different spectra are arbitrarily shifted vertically for clarity. The fall time of the integrat-

ed luminescence was 120 ps. Luminescence spectra at lower excitation power are displayed in Fig. 2.

### III. DETERMINATION OF THE CARRIER TEMPERATURE

Two very different approaches to determine the carrier temperature have been used in the literature. In the first method, the high-energy tail of the luminescence lines has been analyzed in the frame of noninteracting quasiparticles.<sup>5-12</sup> The complete line shape is described by

$$I(h\nu) = C_1 (h\nu - E_g^0)^{1/2} f_e \left[ \frac{m_h}{M} (h\nu - E_G) \right] \times f_h \left[ \frac{m_e}{M} (h\nu - E_G) \right], \quad (1)$$

where  $f_e$  and  $f_h$  are Fermi-Dirac distributions and  $m_e$  and  $m_h$  masses of electrons and holes, respectively.  $M$  is the excitonic translation mass. The gap energy  $E_g^0$  depends only on the lattice temperature  $T_L$ . Constants are denoted by  $C_1$ . The high-energy tail can be well approximated by a simple exponential of the form

$$I(h\nu) \approx \exp(-h\nu/k_B T_{\text{eff}}), \quad (2)$$

where  $T_{\text{eff}}$  is an effective temperature related to the electron and hole temperatures by the following relation:

$$\frac{m_e + m_h}{T_{\text{eff}}} = \frac{m_h}{T_e} + \frac{m_e}{T_h}. \quad (3)$$

Usually it is assumed that  $T_e = T_h$ , so that  $T_{\text{eff}} = T_e = T_h = T_c$  is the common carrier temperature.

In the second method, the whole line shape has been fitted using a many-particle approach.<sup>14,15,18-23</sup> A general formula for the spontaneous recombination in a plasma including any form of state broadening reads

$$I(h\nu) = C_2 \int_0^{+\infty} f_e(k) f_h(k) \frac{\Gamma(k, h\nu)}{\left[ h\nu - E_g(\rho, T_c) - \frac{\hbar^2 k^2}{2\mu} \right]^2 + \Gamma^2(k, h\nu)} k^2 dk, \quad (4)$$

where  $\mu$  is the reduced excitonic effective mass and  $\Gamma(k, h\nu)$  describes a general collision broadening which is often also called damping. Now the energy band gap  $E_g$  additionally depends on the density  $\rho$  and the temperature  $T_c$  of the plasma. The gap shrinkage  $\Delta E_g$  measured in Rydberg energy  $R_H$  can be approximated in the following way:<sup>16</sup>

$$\frac{\Delta E_g}{R_H} = - \frac{4.64 (\rho a_B^3)^{0.5}}{\left[ \rho a_B^3 + \left[ \frac{0.1 k_B T_c}{R_H} \right]^2 \right]^{0.25}}, \quad (5)$$

where  $a_B$  is the excitonic Bohr radius. In the limit  $T_c = 0$ , Eq. (5) reduces to  $\Delta E_g/R_H = -4.64 (\rho a_B^3)^{+0.25}$ ,

leading to numerical values of the band-gap renormalization very close to the data published by Vashista and Kalita.<sup>24</sup>

Landsberg first introduced a collision broadening in order to explain the luminescence tail observed for  $h\nu < E_g$ ,<sup>14</sup> which would be impossible according to Eq. (1). We want to stress now that, following more recent many-body treatments of the collision broadening, the high-energy tail of the luminescence may also be strongly affected and that Eq. (2) does not always give the correct plasma temperature. We follow the model developed by Haug and Tran Thoai<sup>15</sup> which includes (i) collision lifetime broadening of the electron and hole states in direct optical transitions in  $k$  space where the states are

broadened by fast emission or reabsorption of plasmons, (ii) indirect transitions involving plasmon emission or absorption, and (iii) finite lifetime of the plasmons, or plasmon damping, due to intervalence-band absorption in the plasmon-pole approximation. The damping  $\Gamma(k, h\nu)$  in Eq. (4) reads

$$\Gamma_{e,h}^{\pm}(k, h\nu) = \frac{e^2 \hbar^2 \omega_{\text{pl}}^2(0)}{2\pi\epsilon_0} \int_0^{+\infty} \frac{dq}{\hbar\omega_{\text{pl}}(q)} \int_{-1}^{+1} \frac{\Delta(q)}{[h\nu - E_{e,h}(k^2 - 2qk\varphi + q^2) \pm \hbar\omega_{\text{pl}}(q)]^2 + \Delta^2(q)} \times \{b[h\nu - E_{e,h}(k^2 - 2qk\varphi + q^2)] + 1 - f_{e,h}(k^2 - 2qk\varphi + q^2)\} d\varphi, \quad (7)$$

where the plasmon dispersion law  $\hbar\omega_{\text{pl}}(q)$  is approximately given in the plasmon-pole approximation by

$$\hbar^2\omega_{\text{pl}}^2(q) = \hbar^2\omega_{\text{pl}}^2(0) - \hbar^2\Delta_0^2 + \hbar^2\omega_{\text{pl}}^2(0) \left[ \frac{q^2}{q_D^2} \right] + \frac{1}{4} \left[ \frac{\hbar^2}{2\mu} q^2 \right]^2. \quad (8)$$

$\hbar^2\omega_{\text{pl}}^2(0)$  is the square of the usual plasmon energy given by  $\hbar^2\omega_{\text{pl}}^2(0) = 4\pi\rho e^2/\epsilon_0\mu$ .  $q_D$  is the Debye-Hückel wave vector which reads

$$q_D^2 = -\frac{4\pi e^2}{\epsilon_0} \sum_{k,\lambda} \left[ \frac{\partial f_{\lambda}(k)}{\partial E_{\lambda}(k)} \right].$$

The plasmon damping  $\Delta(q)$  is given by

$$\Delta^2(q) = \hbar^2\Delta_0^2 + \frac{1}{4} \left[ \frac{\hbar^2}{2\mu} q^2 \right]^2. \quad (9)$$

The damping constant  $\hbar^2\Delta_0^2$  describes the strength of the intravalence-band absorption of plasmons at the center of the Brillouin zone. In our calculations we used  $\Delta_0 = (0.1-0.2)\omega_{\text{pl}}(0)$ . Figure 3 displays several examples of collision broadening as a function of wave vector  $k$  calculated for CdTe using the parameters of Table I. Figure 3(a) shows the results at high temperature, Fig. 3(b) at low temperature and for two different densities, respectively. At low densities and high temperature, i.e., for nondegenerate plasmas, the electron and the hole damping depend only slightly on the wave vector [dotted and solid lines in Fig. 3(a)]. At high density and low temperature, the electron damping goes almost to zero at the Fermi wave vector [solid and dashed lines in Fig. 3(b)], as in the early Landsberg approach, but then it rises again at a larger wave vector to several meV corresponding to several tens of kelvin. This implies that the shape of the high-energy tail of the luminescence spectra must be changed by damping when the EHP becomes degenerate, especially at high density and low temperature. For instance, in Fig. 3(b) the effect of damping broadening ( $\Gamma \geq 4-5$  meV) exceeds the effect of temperature ( $k_B T_c = 1.7$  meV). The folding of the high-energy tail with a Lorentzian-shaped damping function, as described by Eq. (4), then transfers intensity from higher- to lower-intensity regions. As a result, the temperatures deduced

$$\Gamma(k, h\nu) = \Gamma_e^+(k, E_e) - \Gamma_e^-(k, E_e) + \Gamma_h^+(k, E_h) - \Gamma_h^-(k, E_h), \quad (6)$$

where  $E_{e,h}$  denotes the kinetic energy of electrons and holes.  $\Gamma_{e,h}^{\pm}$  is given by the following double integral:<sup>15</sup>

from the semilogarithmic plot of  $I(h\nu)$  according to Eq. (2) are always too high.

The dotted points in Figs. 1 and 2 are fits to the experimental spectra according to the damping theory described above with the density and the temperature as adjustable parameters. The band-gap renormalization, which is responsible for the shift of the whole luminescence line toward lower energy, is determined from Eq. (5) and in principle ought not to be adjustable. Nevertheless, this was not fully possible and we had to increase slightly the gap shrinkage predicted by Eq. (5) as will be discussed in Sec. V. The low-energy tail is reproduced best only for the highest densities and temperatures (uppermost curve in Fig. 1).

The temperatures deduced in this way are compared (solid symbols in Fig. 4) with the temperatures which are obtained by a single exponential fit to the high-energy tail (open symbols). The latter are, as expected, always appreciably higher than the former. Similar results have been implicitly obtained in Refs. 18 and 19 for  $\text{Al}_x\text{Ga}_{1-x}\text{As}$  compounds.

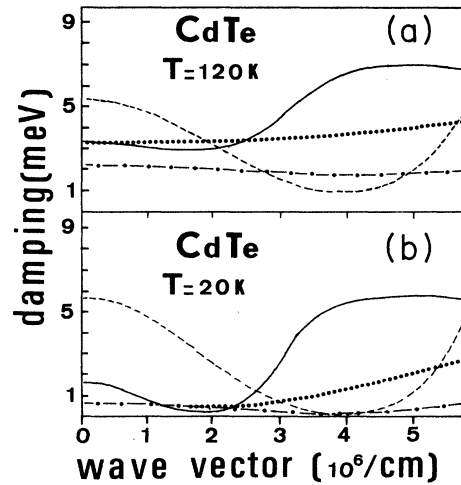


FIG. 3. Electron and hole dampings in CdTe at high plasma density. Plasma density  $2 \times 10^{17}/\text{cm}^3$ : ●●●, hole damping; —, electron damping. Plasma density  $2 \times 10^{18}/\text{cm}^3$ : ●-●, hole damping, - - -, electron damping.

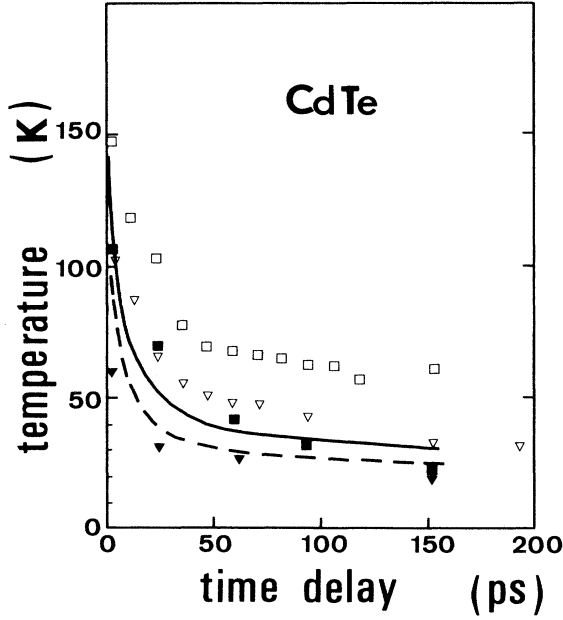


FIG. 4. Plasma temperature kinetics. Plasma temperature deduced from Fig. 1 (higher density):  $\square$  denotes a free-particle model;  $\blacksquare$  denotes a many-particle model. Plasma temperature deduced from Fig. 2 (lower density):  $\nabla$  denotes a free-particle model;  $\blacktriangledown$  denotes a many-particle model. Plasma temperature deduced from Eqs. (10): Solid line denotes initial density  $\rho \approx 4 \times 10^{17}/\text{cm}^3$ ; dashed line denotes initial density  $\rho \approx 0.85 \times 10^{17}/\text{cm}^3$ .

#### IV. COMPARISON WITH PLASMA COOLING THEORY

We summarize briefly the model used to calculate the plasma temperature kinetics. A detailed description of the calculation is reported elsewhere.<sup>25,26</sup> We use three coupled differential equations, one for the conduction electrons, one for the holes, and one for the LO phonons:

$$\begin{aligned}
 \frac{1}{\rho} \frac{d\langle E_e \rangle}{dt} &= -\frac{1}{\rho} \frac{d\langle E_e \rangle}{dt} \Big|_h - \sum_{\alpha} \frac{1}{\rho} \frac{d\langle E_e \rangle}{dt} \Big|_{\alpha} \\
 &\quad + [h\nu - E_g(\rho, T_c)] \frac{m_h}{M} g(t), \\
 \frac{1}{\rho} \frac{d\langle E_h \rangle}{dt} &= \frac{1}{\rho} \frac{d\langle E_e \rangle}{dt} \Big|_h - \sum_{\alpha} \frac{1}{\rho} \frac{d\langle E_h \rangle}{dt} \Big|_{\alpha} \\
 &\quad + [h\nu - E_g(\rho, T_c)] \frac{m_e}{M} g(t), \\
 \frac{dn_{\text{LO}}(q)}{dt} &= \frac{dn_{\text{LO}}(q)}{dt} \Big|_e + \frac{dn_{\text{LO}}(q)}{dt} \Big|_h \\
 &\quad - \frac{n_{\text{LO}}(q) - n_{\text{LO}}^{T_L}}{\tau_{\text{LO}}},
 \end{aligned} \tag{10}$$

where  $g(t)$  is the electron-hole pair generation rate and  $n_{\text{LO}}(q)$  is the phonon occupation at wave vector  $q$  with  $n_{\text{LO}}^{T_L}$  being the occupation corresponding to the lattice temperature.  $\tau_{\text{LO}}$  is the phonon lifetime. The energy-transfer rate

$$\frac{1}{\rho} \frac{d\langle E_e \rangle}{dt} \Big|_h$$

from electrons to holes is outlined in the Appendix and numerical results are given in separate publications.<sup>25,26</sup> The computations show that for the present plasma densities larger than  $10^{16} \text{ cm}^{-3}$  the electron and hole temperatures are almost equal within a few picoseconds. So we restrict for the following analysis on a common carrier temperature. The carrier-energy relaxation by phonon emission is taken into account by the terms

$$\sum_{\alpha} \frac{1}{\rho} \frac{d\langle E_h \rangle}{dt} \Big|_{\alpha}$$

in Eq. (10) where  $\alpha$  stands for the different phonon-emission processes. The details are already explained in Ref. 27. In principle, the emission of LO phonons ought to be screened dynamically for the density range of our experiments, i.e.,  $4 \times 10^{16} \text{ cm}^{-3} < \rho < 4 \times 10^{17} \text{ cm}^{-3}$ , because the LO-phonon energy is close to that of the plasmon. In CdTe, the resonance of the LO-phonon energy with that of plasmons takes place at a density of  $\rho \approx 2.5 \times 10^{17} \text{ cm}^{-3}$ . Nevertheless, we have demonstrated in Ref. 28 that an unscreened Fröhlich interaction can be used to compute the net energy-loss rate by LO-phonon emission

$$\frac{1}{\rho} \frac{d\langle E_{e,h} \rangle}{dt} \Big|_{\text{LO}},$$

at least as long as the LO-phonon distribution is thermalized. (See also Ref. 29.) So we do not screen the LO-phonon interaction to save computation time. The third equation for LO phonons was previously derived and discussed extensively by Pötz and Koccevar.<sup>30</sup> We use the material parameters listed in Table I and a LO-phonon lifetime of  $\tau_{\text{LO}} = 15 \text{ ps}$ .<sup>31</sup> The electron-hole pair generation rate  $g(t)$  is assumed to have a Gaussian profile with a FWHM of 6 ps. The results of the numerical simulations are displayed together with the experimental data in Fig. 4. *It must be stressed that critical parameters such as the phonon lifetime and the plasma density are not adjustable in the cooling theory.* The phonon lifetime is known from Ref. 31. The plasma density is derived directly from the line-shape fit so that we carry out a self-consistent test of both the line-shape theory and of the cooling theory. The temperature for long time ( $100 \text{ ps} < t < 150 \text{ ps}$ ) tends to 20–30 K (solid line and dashed line, Fig. 4). This is a direct consequence of the small LO-phonon energy of 21 meV in CdTe. For comparison, the LO-phonon energy is about 36 meV in GaAs and the asymptotic temperature on the same time scale is then typically 40–50 K. As a consequence, cooling by polar-optical scattering is faster in CdTe than in GaAs and  $\text{Al}_x\text{Ga}_{1-x}\text{As}$  compounds. The fit of the temperature

decay kinetics may be considered as satisfactory considering the large number of experimental parameters involved in the theory (see Table I) and that neither the plasma density nor the phonon lifetime were adjusted. Slight discrepancies also persist on GaAs.<sup>25</sup> The theoretical temperature deduced from plasma equations (10) decays for long time slightly slower than the temperature deduced from the line-shape analysis. Two possible reasons may be invoked.

(a) The plasmon-pole approximation of the random-phase approximation might slightly overestimate dampings especially at low plasma density. In that case, the temperatures deduced from the many-body line-shape analysis might be slightly too low.

(b) The plasma density decay (especially significant for long time) has not been included in the plasma kinetic equations. It would be necessary to add one more kinetic equation in the system (10) for the plasma density. The density relaxation implies a decay of screening of the acoustical-phonon emission and therefore a faster temperature cooling predicted by the theoretical model at long delay.

We must stress that for CdTe the discrepancy between experiments and theory is considerably reduced if the experimental temperatures are evaluated using a many-body line-shape theory, whereas the disagreement remains very important if the plasma temperature is evaluated in the frame of the free-particle model.

## V. BAND-GAP RENORMALIZATION

The band-gap shrinkage obtained from the line fits of Figs. 1 and 2 is compared in Fig. 5 to the theoretical result calculated from Eq. (5). As we already emphasized in Sec. III, we had to increase slightly the theoretical band-gap renormalization predicted by Eq. (5), typically by 3–5 meV, in order to get the best fits. Theory seems

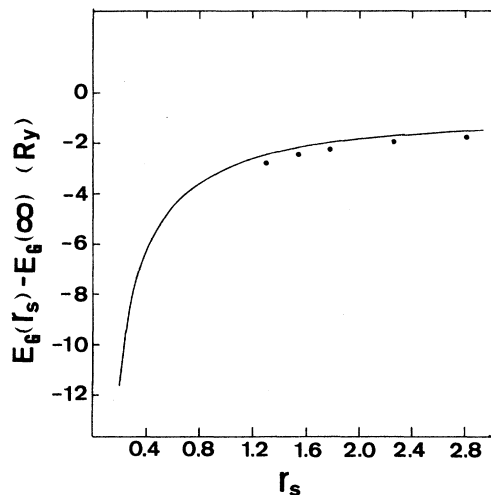


FIG. 5. Band-gap renormalization in the presence of a dense electron-hole plasma. The density is measured in the mean interparticle distance  $r_s$ , defined by  $r_s = (3/4\pi n a_B^3)^{1/3}$ .<sup>33</sup> Solid line: Zimmermann's theory, experimental values.

to underestimate the shrinkage at all densities. This discrepancy may be attributed to a supplementary reduction of the band gap in polar materials due to the interaction with LO phonons.<sup>32</sup> This effect is not included in Eq. (5). The overall agreement of our results with Zimmermann's theory<sup>16</sup> must be considered as good; in particular, the density dependence is the same for experiment and theory. This is also in accordance with similar results on  $\text{Al}_x\text{Ga}_{1-x}\text{As}$ .<sup>33</sup>

## VI. CONCLUSION

This work is, to our knowledge, the first study of the picosecond dynamics of a photogenerated electron-hole plasma in CdTe. The deduction from experimental data of the transient temperatures and plasma densities are, in contrast to previous works, done in the framework of a line-shape theory which includes important many-body effects. This enables us to test simultaneously the plasma cooling theory, the many-body line-shape theory, the carrier damping, and the band-gap renormalization. No parameter is adjustable in the cooling theory. We obtain a satisfactory agreement between experiment and theory for plasma densities ranging from  $5 \times 10^{16} \text{ cm}^{-3}$  to  $4 \times 10^{17} \text{ cm}^{-3}$ . On the contrary, an important and unresolved disagreement between the experiment and the theory persists if the plasma temperature is deduced from the luminescence line shape in the frame of the usual free-particle model.

The cooling due to polar-optical scattering is in CdTe much faster than in III-V materials as, e.g., GaAs since the LO-phonon energy of 21 meV is rather small.

## ACKNOWLEDGMENTS

This work was supported by a contract from the Direction des Recherches et Etudes Techniques (DGA). The Laboratoire de Physique Solides, Institut National des Sciences, is Unité associé au Centre National de la Recherche Scientifique.

## APPENDIX: GENERAL EXPRESSION OF THE ENERGY-TRANSFER RATE BY ELECTRON-HOLE COLLISIONS

One idea which explains the discrepancy between experiment and theory on cooling of EHP is that electrons and holes may have for long times (50–100 ps) different temperatures, say the electrons are typically 10 K hotter than the holes.<sup>25,26,34</sup> Then, the cooling of holes by polar-optical scattering would be much less efficient than that of electrons. The temperature difference could help to reduce the theoretical cooling rate at higher densities, since for electrons a nonthermal phonon population is very easily reached whereas for holes this would require much higher densities. There exist already several publications which assume differences between electron and hole temperatures.<sup>33,34</sup> Here we derive the general expression of the energy transfer rate from electrons to holes in order to complete our previous derivations of the energy-loss rates by phonon emission.<sup>27,28</sup> Our result is more general than that of Refs. 34 and 35 and holds in

degenerate as well as in nondegenerate conditions.

Let us consider the following scattering process: One electron is scattered from the wave vector  $\mathbf{k}_e$  to the wave vector  $\mathbf{k}_e - \mathbf{q}$  and a hole is scattered from the vector  $\mathbf{k}_h$  to the vectors  $\mathbf{k}_h + \mathbf{q}$ . The energy exchanged between the two particles in the collision process is

$$\begin{aligned} \Delta E(\mathbf{k}_e, \mathbf{k}_h, \mathbf{q}) &= E(k_e) - E(\mathbf{k}_e - \mathbf{q}) \\ &= E_h(\mathbf{k}_h + \mathbf{q}) - E_h(k_h) \\ &= \frac{\hbar^2}{m_e} q k_e \cos\theta - \frac{\hbar^2}{2m_e} q^2 \\ &= \frac{\hbar^2}{m_h} q k_h \cos\theta' + \frac{\hbar^2}{2m_h} q^2. \end{aligned} \quad (\text{A1})$$

Here,  $\theta$  ( $\theta'$ ) is the angle between the vectors  $\mathbf{k}_e$  and  $\mathbf{q}$  ( $\mathbf{k}_h$  and  $\mathbf{q}$ ). If  $\Delta E$  is positive, the electron loses kinetic energy. The transition probability for this process is

$$\begin{aligned} P(\mathbf{k}_e, \mathbf{k}_h, \mathbf{q}) &= \frac{2\pi}{\hbar} \left| \frac{V_0(\mathbf{k}_e, \mathbf{k}_h, \mathbf{q})}{\epsilon(q, \Delta E)} \right|^2 \\ &\quad \times \delta(E(k_e) - E(\mathbf{k}_e - \mathbf{q}) \\ &\quad - E_h(\mathbf{k}_h + \mathbf{q}) - E_h(k_h)), \end{aligned} \quad (\text{A2})$$

where  $V_0(\mathbf{k}_e, \mathbf{k}_h, \mathbf{q})$  is the scattering amplitude and  $\epsilon(q, \Delta E)$  is the plasma dielectric function. The  $\delta$  function

$$\begin{aligned} \frac{dE(\xi)}{dt} \Big|_{eh} &= \sum_q \Delta E [1 - f_e(\xi - \Delta E)] \left| \frac{V_0(q)}{\epsilon(q, \Delta E)} \right|^2 \frac{1}{4\pi^2 \hbar} \left[ \frac{2m_h}{\hbar^2} \right]^{3/2} \\ &\quad \times \int_0^\infty \sqrt{\lambda} d\lambda \int_{-1}^{+1} d\varphi' f_h(\lambda) [1 - f_h(\lambda + \Delta E)] \delta(2\varphi' \sqrt{\xi} \eta - \eta - 2\varphi' \sqrt{\lambda/\sigma} \eta - \eta/\sigma). \end{aligned} \quad (\text{A5})$$

Here  $\sigma = m_h/m_e$ . The contribution of the integration over  $\varphi'$  is equal to  $\frac{1}{2} \sqrt{\sigma/\lambda} \eta$  if the equation  $2\varphi' \sqrt{\xi} \eta - \eta - 2\varphi' \sqrt{\lambda/\sigma} \eta - \eta/\sigma = 0$  has one solution ( $\lambda, \varphi'$ ) with  $-1 < \varphi' < 1$ . This becomes possible as soon as  $\lambda$  is larger than

ensures energy conservation. The energy exchanged per second by the  $\mathbf{k}$  electron is

$$\begin{aligned} \frac{dE(\mathbf{k})}{dt} \Big|_{eh} &= \sum_q \Delta E(\mathbf{k}_e, \mathbf{k}_h, \mathbf{q}) [1 - f_e(\mathbf{k}_e - \mathbf{q})] \\ &\quad \times \sum_{k_h, \sigma_h} P(\mathbf{k}_e, \mathbf{k}_h, \mathbf{q}) f_h(\mathbf{k}_h) \\ &\quad \times [1 - f_h(\mathbf{k}_h + \mathbf{q})]. \end{aligned} \quad (\text{A3})$$

The average energy exchanged (per particle) between electrons and holes reads simply

$$\frac{1}{\rho} \frac{d\langle E \rangle}{dt} \Big|_{eh} = \frac{1}{\rho} \sum_{k, \sigma_e} f_e(\mathbf{k}) \frac{dE(\mathbf{k})}{dt} \Big|_{eh}, \quad (\text{A4})$$

where  $\rho$  is the plasma density. We use the simple scattering amplitude  $V_0(\mathbf{k}_e, \mathbf{k}_h, \mathbf{q}) = V_0(q) = 4\pi e^2 / \epsilon_0 q^2$  and assume isotropic bands. We rewrite the exchanged energy  $\Delta E$  [Eq. (A1)] as follows:  $\Delta E = \Delta E(\xi, \eta, \varphi) = 2\varphi \sqrt{\xi} \eta - \eta$ . We use  $\xi = (\hbar^2/2m_e) k^2$  (the initial energy of the electron),  $\eta = (\hbar^2/2m_e) q^2$ , and  $\varphi = \cos(\theta)$ . We write  $f_e(\xi)$  instead of  $f_e(\mathbf{k})$ , and  $f_e(\xi - \Delta E)$  instead of  $f_e(\mathbf{k}_e - \mathbf{q})$ . For the holes, we replace  $f_h(\mathbf{k}_h)$  and  $f_h(\mathbf{k}_h + \mathbf{q})$  by  $f_h(\lambda)$  and  $f_h(\lambda + \Delta E)$ , respectively, where  $\lambda$  is the hole initial kinetic energy. Let us first calculate  $dE(\mathbf{k})/dt|_{eh}$ . Introducing continuous coordinates, we get

$$\lambda_0 = \frac{1}{\sigma} \left| \sigma \varphi \sqrt{\xi} - \frac{\sigma + 1}{2} \sqrt{\eta} \right|^2.$$

This condition reduces to  $[\lambda_0, +\infty]$  the integration interval over  $\lambda$ . We deduce

$$\frac{dE(\xi)}{dt} \Big|_{eh} = \sum_q \Delta E [1 - f_e(\xi - \Delta E)] \left| \frac{V_0(q)}{\epsilon(q, \Delta E)} \right|^2 \frac{\sqrt{2} m_h^{3/2}}{\pi \hbar^4} \int_{\lambda_0}^\infty \sqrt{\lambda} \frac{1}{2} \sqrt{\sigma/\lambda} \eta d\lambda f_h(\lambda) [1 - f_h(\lambda + \Delta E)]. \quad (\text{A6})$$

Introducing now continuous coordinates for the  $q$  summation,  $dE(\xi)/dt|_{eh}$  reads, after a little algebra,

$$\begin{aligned} \frac{dE(\xi)}{dt} \Big|_{eh} &= \frac{1}{8\pi^3} \left[ \frac{2m_e}{\hbar^2} \right]^{3/2} \int_0^\infty \frac{d\eta}{2} \int_{-1}^{+1} d\varphi \int_{\lambda_0}^\infty d\lambda \Delta E [1 - f_e(\xi - \Delta E)] \left| \frac{V_0(q)}{\epsilon(q, \Delta E)} \right|^2 \\ &\quad \times \frac{m_h^2}{\pi \hbar^4 \sqrt{2m_e}} \int_{\lambda_0}^\infty d\lambda f_h(\lambda) [1 - f_h(\lambda + \Delta E)]. \end{aligned} \quad (\text{A7})$$

Static screening of the electron-hole collision is an excellent approximation if the masses of electrons and holes are very different (see the Appendix of Ref. 27). So we use the static limit  $\epsilon(q, \Delta E) = 1 + q_D^2/q^2$  in Eq. (A7) where  $q_D$  is the Debye-Hückel screening wave vector defined by

$$q_D^2 = -\frac{4\pi e^2}{\epsilon_0} \sum_{k,\lambda} \left[ \frac{\partial f_\lambda(k)}{\partial E_\lambda(k)} \right].$$

In case of thermalized regime, the integration over  $\lambda$  can be calculated analytically and we get the following formula:

$$\left. \frac{dE(\xi)}{dt} \right|_{eh} = S \int_0^\infty \frac{d\rho}{|\eta + \eta_D|^2} \int_{-1}^1 d\varphi \Delta E \frac{1 - f_e(\xi - \Delta E)}{\exp\left[\frac{-\Delta E}{k_B T_h}\right] - 1} \ln \left[ \frac{1 + \exp\left[\frac{-\lambda_0 + \mu_h}{k_B T_h}\right]}{1 + \exp\left[\frac{-\lambda_0 - \Delta E + \mu_h}{k_B T_h}\right]} \right]. \quad (\text{A8})$$

Here,  $\eta_D = (\hbar^2/2m_e)q_D^2$ ,  $S = m_h^2 e^4 k_B T_h / m_e \pi \hbar^3 \epsilon_0^2$ , and  $\mu_h$  is the Fermi level of holes. Finally, the energy transfer

$$\left. \frac{1}{\rho} \frac{d\langle E \rangle}{dt} \right|_{eh}$$

from electrons to holes reads

$$\left. \frac{1}{\rho} \frac{d\langle E \rangle}{dt} \right|_{eh} = \frac{1}{2\pi^2 \rho} \int_0^\infty \sqrt{\xi} f_e(\xi) \left. \frac{dE(\xi)}{dt} \right|_{eh} d\xi. \quad (\text{A9})$$

Numerical computations show in fact that the electron and hole temperatures for density larger than  $10^{16} \text{ cm}^{-3}$  are very close within a few picoseconds. So the assumption of a common temperature  $T_c$  is well justified in our present experiments.

\*Present address: AT&T Bell Laboratories, Holmdel, NJ 07733.

<sup>1</sup>J. Collet and T. Amand, *Solid State Commun.* **59**, 173 (1986).

<sup>2</sup>J. Collet and M. Pagnet, *Phys. Status Solidi B* **46**, 393 (1988).

<sup>3</sup>H. Schweizer and E. Zielinski, *J. Lumin.* **30**, 37 (1985).

<sup>4</sup>T. Ohtsuki, T. Kushida, S. Hongo, and H. Bo, *J. Phys. Soc. Jpn.* **53**, 4064 (1984).

<sup>5</sup>J. Shah, *Solid-State Electron.* **21**, 43 (1978).

<sup>6</sup>E. O. Göbel and O. Hildebrand, *Phys. Status Solidi B* **88**, 645 (1978).

<sup>7</sup>R. G. Ulbrich, *Phys. Rev. B* **8**, 5719 (1973).

<sup>8</sup>T. Amand and J. Collet, *J. Phys. Chem. Solids* **46**, 1053 (1985).

<sup>9</sup>K. Leo, W. W. Rühle, and K. Ploog, *Phys. Rev. B* **38**, 1947 (1988).

<sup>10</sup>W. W. Rühle, K. Leo, E. Bauser, in *Proceedings of the 19th International Conference on the Physics of Semiconductors*, edited by W. Zawadzki (Institute of Physics, Warsaw, 1989), p. 1399.

<sup>11</sup>H. Lobentanzer, H. J. Polland, W. W. Rühle, W. Stolz, and K. Ploog, *Appl. Phys. Lett.* **51**, 673 (1987).

<sup>12</sup>W. W. Rühle and H. J. Polland, *Phys. Rev. B* **36**, 1683 (1987).

<sup>13</sup>S. A. Lyon, *J. Lumin.* **35**, 121 (1987).

<sup>14</sup>P. T. Landsberg, *Phys. Status Solidi* **15**, 623 (1966).

<sup>15</sup>H. Haug and D. B. Tran Thoai, *Phys. Status Solidi B* **98**, 581 (1980).

<sup>16</sup>R. Zimmermann, *Phys. Status Solidi B* **146**, 71 (1988).

<sup>17</sup>C. Konank, J. Dillinger, and U. Proser, in *Proceedings of the 1967 International Conference on II-VI Semiconductor Compounds*, edited by D. G. Thomas W. A. (Benjamin, New York, 1967), p. 850.

<sup>18</sup>A. Selloni, S. Modesti, and M. Capizzi, *Phys. Rev. B* **30**, 821 (1984).

<sup>19</sup>M. Capizzi, S. Modesti, A. Frova, J. L. Staehli, M. Guzzi, and R. A. Logan, *Phys. Rev. B* **29**, 2028 (1984).

<sup>20</sup>G. Tränkle, H. Leier, A. Forchel, H. Haug, C. Ell, and G. Wiegmann, *Phys. Rev. Lett.* **58**, 419 (1987).

<sup>21</sup>C. Klingshirn and H. Haug, *Phys. Rep.* **70**, 316 (1981).

<sup>22</sup>R. Zimmerman, *Phys. Status Solidi B* **86**, K78 (1978).

<sup>23</sup>K. Arya and W. Hanke, *Phys. Rev. B* **23**, 2988 (1981).

<sup>24</sup>P. Vashista and R. K. Kalia, *Phys. Rev. B* **25**, 6492 (1982).

<sup>25</sup>K. Leo, Ph. D. thesis, University of Stuttgart, 1988.

<sup>26</sup>K. Leo (unpublished).

<sup>27</sup>M. Pagnet, J. Collet, and A. Cornet, *Solid State Commun.* **38**, 531 (1981).

<sup>28</sup>J. Collet, *Phys. Rev. B* **39**, 7659 (1989).

<sup>29</sup>S. Das Sharma, J. K. Jain, and R. Jalabert, *Phys. Rev. B* **37**, 6290 (1988).

<sup>30</sup>W. Pötz and P. Kocevar, *Phys. Rev. B* **28**, 7040 (1983).

<sup>31</sup>D. von der Linde and R. Lambrich, in *Proceedings of the 14th International Conference on the Physics of Semiconductors*, IOP Conf. Proc. Ser. No. 43, edited by B. L. Wilson (IOP, Bristol, 1979).

<sup>32</sup>S. Schmitt-Rink, D. B. Tran Thoai, and H. Haug, *Z. Phys. B* **39**, 25 (1980).

<sup>33</sup>T. F. Boggess, H. Kalt, K. Bohnert, D. P. Norwood, and A. L. Smirl, *Proc. SPIE* **793**, 37 (1987).

<sup>34</sup>M. Asche and O. G. Sarbei, *Phys. Status Solidi B* **141**, 487 (1987).

<sup>35</sup>W. Pötz, *Phys. Rev. B* **36**, 5016 (1987).